

Novel dominant MPAN family with a complex genetic architecture as a basis for phenotypic variability

Peter Balicza, MD, PhD, Renata Bencsik, MSc, Andras Lengyel, MD, Aniko Gal, PhD, Zoltan Grosz, MD, Dora Csaban, MSc, Gabor Rudas, MD, PhD, Krisztina Danics, MD, PhD, Gabor G. Kovacs, MD, PhD, FRCPC, and Maria Judit Molnar, MD, PhD

Correspondence

Dr. Balicza
balicza.peter@
med.semmelweis-univ.hu

Neurol Genet 2020;6:e515. doi:10.1212/NXG.0000000000000515

Abstract

Objective

Our aim was to study a Hungarian family with autosomal dominantly inherited neurodegeneration with brain iron accumulation (NBIA) with markedly different intrafamilial expressivity.

Methods

Targeted sequencing and multiplex ligation-dependent probe amplification (MLPA) of known NBIA-associated genes were performed in many affected and unaffected members of the family. In addition, a trio whole-genome sequencing was performed to find a potential explanation of phenotypic variability. Neuropathologic analysis was performed in a single affected family member.

Results

The clinical phenotype was characterized by 3 different syndromes—1 with rapidly progressive dystonia-parkinsonism with cognitive deterioration, 1 with mild parkinsonism associated with dementia, and 1 with predominantly psychiatric symptoms along with movement disorder. A heterozygous stop-gain variation in the *C19Orf12* gene segregated with the phenotype. Targeted sequencing of all known NBIA genes, and MLPA of *PLA2G6* and *PANK2* genes, as well as whole-genome sequencing in a trio from the family, revealed a unique constellation of oligogenic burden in 3 NBIA-associated genes (*C19Orf12* p.Trp112Ter, *CP* p.Val105PhefsTer5, and *PLA2G6* dup(ex14)). Neuropathologic analysis of a single case (39-year-old man) showed a complex pattern of alpha-synucleinopathy and tauopathy, both involving subcortical and cortical areas and the hippocampus.

Conclusions

Our study expands the number of cases reported with autosomal dominant mitochondrial membrane protein-associated neurodegeneration and emphasizes the complexity of the genetic architecture, which might contribute to intrafamilial phenotypic variability.

From the Institute of Genomic Medicine and Rare Diseases (P.B., R.B., A.L., A.G., Z.G., D.C., M.J.M.), Semmelweis University, Budapest, Hungary; Neurology Outpatient Clinic (A.L.), General Medical Clinic, Motala Hospital, Sweden; Department of Neuroradiology (G.R.), and Department of Forensic and Insurance Medicine (K.D.), Semmelweis University, Budapest, Hungary; Tanz Centre for Research in Neurodegenerative Disease (G.G.K.), and Department of Laboratory Medicine and Pathobiology (G.G.K.), University of Toronto; and Laboratory Medicine Program (G.G.K.), University Health Network, Toronto, Canada.

Go to [Neurology.org/NG](https://www.neurology.org/NG) for full disclosures. Funding information is provided at the end of the article.

The Article Processing Charge was funded by the Hungarian Brain Research Program.

This is an open access article distributed under the terms of the Creative Commons Attribution-NonCommercial-NoDerivatives License 4.0 (CC BY-NC-ND), which permits downloading and sharing the work provided it is properly cited. The work cannot be changed in any way or used commercially without permission from the journal.

Glossary

APP = amyloid precursor protein; **MLPA** = multiplex ligation-dependent probe amplification; **MPAN** = mitochondrial membrane protein-associated neurodegeneration; **NBIA** = neurodegeneration with brain iron accumulation; **WGS** = whole-genome sequencing.

Neurodegeneration with brain iron accumulation (NBIA) is a group of rare, heterogeneous, hereditary neurodegenerative diseases in which excess iron accumulates in the basal ganglia and other vulnerable brain areas.¹ At least 10 known genes are clearly associated with the condition²: *ATP13A2*, *C19Orf12*, *COASY*, *CP*, *DCAF17*, *FA2H*, *FTL*, *PANK2*, *PLA2G6*, and *WDR45*. Clinical differentiation between different types of NBIA is often very difficult because of the pleiotropy of the causative genes.

Mitochondrial membrane protein-associated neurodegeneration (MPAN) is a form of neurodegeneration with brain iron accumulation (NBIA-4; MIM614298) caused by pathogenic variants in the *C19Orf12* gene. Although the study on the first family with MPAN reports it as an autosomal recessive condition,³ dominant inheritance of the disease was confirmed recently.⁴ Independent of the inheritance pattern, most MPAN cases are phenotypically similar at both clinical and neuropathologic levels.⁴

In this article, we report a novel large family with autosomal dominantly inherited NBIA associated with a segregating stop-gain variant in the *C19Orf12* gene. Targeted sequencing and multiplex ligation-dependent probe amplification (MLPA) of other NBIA genes and whole-genome sequencing in a trio from the family revealed a unique constellation of

oligogenic burden in 3 NBIA-associated genes. Neuropathologic analysis of a single case showed a complex pattern of alpha-synucleinopathy and tauopathy.

Methods

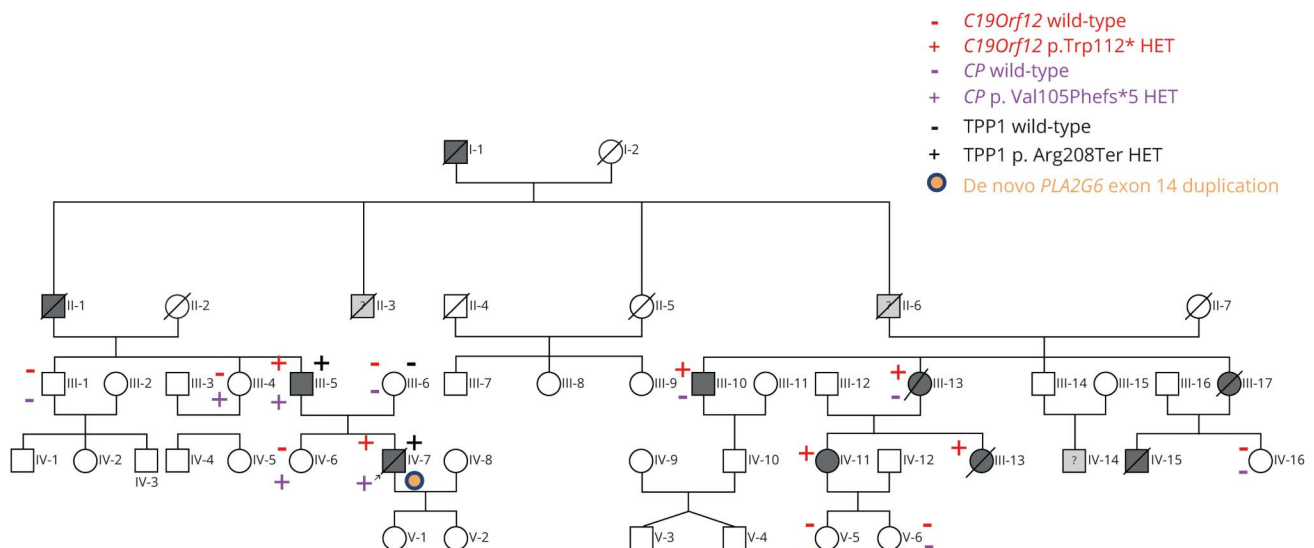
Clinical evaluation

Six members of the family (figure 1) (originating from Hungary) were examined by board-certified neurologists (A.L., P.B., M.J.M., and Z.G.) in the last 10 years at 2 academic centers (Debrecen and Budapest). For further 6 family members, medical documents from other centers and blood samples were available for this study. Brain MRIs, which are shown in this study, were performed on a 3T MRI, and the images were analyzed by a neuroradiologist (R.G.). This article presents a retrospective case study conducted with the approval from the institutional ethical committee. All participants provided informed written consent for the genetic studies.

Genetic analysis

Genetic investigations were performed from blood isolated with the Qiagen Blood Mini Kit. Sanger sequencing was performed for *C19ORF12*, *CP*, *PANK2*, *PLA2G6*, *COASY*, and *BPAN* genes. Whole-genome sequencing was

Figure 1 Family tree



Genetically examined patients are marked on the family tree by a plus or minus sign, whereas color codes are used for different genetic variants. The index case is indicated with an arrow sign. Neurologic examinations performed by the authors were carried out in patients III/3, III/6, III/10, IV/7, IV/11, V/5, and V/6.

performed in a trio at Novogene (en.novogene.com/), whereas data analysis from the whole-genome sequencing (WGS) was performed at the Institute of Genomic Medicine and Rare Disorders Semmelweis University (P.B.). Alignment was performed with Burrows-Wheeler Aligner (BWA-MEM), whereas variant calling was performed with the GATK haplotype caller. Multiple softwares were used for variant filtration, namely Genesis application (genesis-app.com), TGex (tgex.genecards.org), Moon software (diploid.com/moon) and the in-house software Variant-Analyzer. We also performed copy number variation call from the WGS data set using the CNVkit WGS method. MLPA was performed with the SALSA MLPA P120 probemix kit, which covers the *PANK2* and *PLA2G6* genes. The detailed filtration process is available in appendix e-1 (links.lww.com/NXG/A318).

Neuropathology

Formalin-fixed, paraffin-embedded tissue blocks were evaluated. In addition to hematoxylin and eosin and Luxol Fast Red staining, the following monoclonal antibodies were used for immunohistochemistry: anti- τ AT8 (pS202/pT205, 1:200; Pierce Biotechnology, Rockford, IL), anti-phospho-TDP-43 (pS409/410, 1:2,000; Cosmo Bio, Tokyo, Japan), anti- α -synuclein (1:2,000, clone 5G4; Roboscreen, Leipzig, Germany), anti-A β (1:50, clone 6F/3D; Dako, Glostrup, Denmark), and anti-amyloid precursor protein (APP, 1:8,000; Millipore, Burlington, MA). The DAKO EnVision detection kit (peroxidase/DAB, rabbit/mouse) was used for visualization of antibody. Neuropathologic alterations in all examined anatomic regions were evaluated semiquantitatively (as none, mild, moderate, and severe).

Data availability

The data sets used and/or analyzed during the current study are available from the corresponding author on reasonable request.

Results

Family history and clinical phenotype

The family history showed an autosomal dominant pattern (figure 1). We have examined 6 members of the family and collected information and blood sample from 6 further family members. Three different clinical syndromes were observed (table):

First, rapidly progressive dystonia-parkinsonism with dementia was present in the index case (IV/7) and in patient IV/15. In the index case (IV/7), symptoms started around age 30 years, and he died at age 39 years. Wilson disease was first suspected in another center because serum ceruloplasmin and copper repeatedly decreased, but genetic testing of *ATP7B* was negative, and MRI suggested iron accumulation in the basal ganglia. Because of the diagnostic

uncertainty, liver biopsy was also performed earlier, which did not identify copper accumulation. Post hoc examination of the MRI also confirmed linear T2 hyperintensity at the medial medullary lamina of the globus pallidus. Examination at age 39 years detected severe parkinsonism, supranuclear vertical gaze palsy, generalized dystonia, severe dysphagia, widespread pyramidal tract signs, and dementia. At this late stage, ophthalmologic examination showed retinal dysfunction; however, optic atrophy was not described. Patient IV/15 presented with childhood-onset gait impairment and mental decline with initially slow progression and secondary rapid deterioration in his last 3 years. Parkinsonism was first appreciated at age 36 years. In the next year, rapid neurologic deterioration started, and at age 39 years, when he died of a concomitant pneumonia, severe dystonia-parkinsonism with dementia was present. Pathologic examination of the liver was normal. Genetic studies could not be performed from the available post-mortem formalin-fixed paraffin-embedded brain samples because of pronounced DNA degradation. Brain neuropathology was partially reported earlier,⁵ which was expanded in this study after the genetic diagnosis was made in other family members.

Second, relatively mild, late-onset, slowly progressive parkinsonism and cognitive decline were present in the father of the index case (III/5) and his cousin (III/10).

Third, psychiatric symptoms along with mild movement disorder were observed in patient IV/11. She showed signs of mild disinhibition and abnormal results in the Luria test. Detailed neuropsychiatric examination detected mild frontotemporal cognitive decline. Fundus examination did not detect optic atrophy at age 46 years. Although her daughter (V/5) was diagnosed with schizophrenia, we do not attribute this to MPAN because genetic and MRI studies were negative. Reportedly, other female family members (patients III/13, III/17, and IV/13) had also predominant psychiatric symptoms.

Brain MRI findings

Brain MRIs (figure 2) revealed classical signs of brain iron accumulation; however, well-identifiable differences such as atypical iron accumulation in the caudate, together with cortical atrophy in patient III/10 and frontal atrophy in patient IV/1, have also been detected in different family members.

Genetic analysis

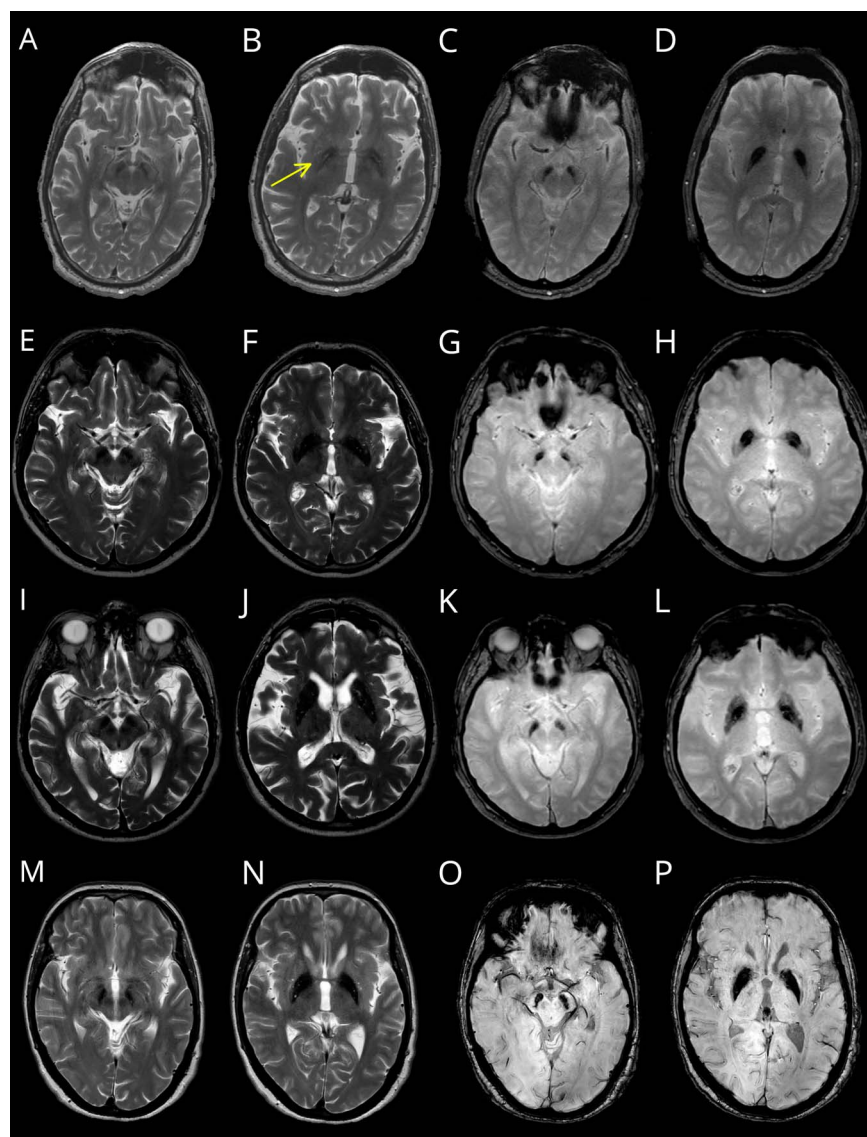
Sanger sequencing of *PANK2*, *PLA2G6*, *CP*, and *C19Orf12* was performed in the index case (IV.7), which identified a heterozygous nonsense variant in the *C19Orf12* gene (NM_001031726.3:c.335G>A; p.Trp112Ter) and a heterozygous deletion in the *CP* gene, causing a frameshift (c.313delG, p.Val105Phefs*5). WGS trio sequencing identified a further, heterozygous *TPPI* stop-gain variant (NM_000391.4:c.622C>T; p.Arg208Ter) inherited from the father, and

Table Phenotype and genotype information of the family members

Patient	Examined by us	Main symptoms	Age at onset, y	MRI	C19Orf12 p.Trp112Ter	CP p.Val105PhefsTer5	TPP1 p.Arg208Ter	PLA2G6 dup(ex14)
III/1	No	No symptoms	N/A	Not performed	Negative	Negative	Not tested	Not tested
III/4	No	No symptoms	N/A	Not performed	Negative	Positive	Not tested	Not tested
III/5	Yes	Mild parkinsonism (MOCA = 27)	Unknown (examined at age 63 y)	Iron accumulation in the GP and SN	Positive	Positive	Positive	Negative
III/6	Yes	No symptoms	N/A	Not performed	Negative	Negative	Negative	Negative
III/10	Yes	Mild parkinsonism and cognitive decline (MOCA = 25)	Late onset (~60 y)	Iron accumulation in the GP, putamen, caudate nucleus, and SN	Positive	Negative	Not tested	Not tested
III/13	No, deceased	Psychiatric symptoms	Unknown	Reportedly positive	Positive	Negative	Not tested	Not tested
III/17	No, deceased	Psychiatric symptoms (depression and suicide)	Unknown	Unknown	Not tested	Not tested	Not tested	Not tested
IV/6	No	No symptoms	N/A	Not performed	Negative	Positive	Not tested	Not tested
IV/7	Yes	Severe dystonia-parkinsonism and dementia	Early onset (~30 y)	Iron accumulation in the GP and SN. Hyperintense streak in the GP	Positive	Positive	Positive	Positive
IV/11	Yes	Mild frontal lobe symptoms (MOCA = 28) and dysdiadochokinesis	Unknown (examined at age 46 y)	Iron accumulation in the GP and SN and mild frontal atrophy	Positive	Not tested	Not tested	Not tested
IV/13	No, deceased	Focal dystonia and psychiatric symptoms	Unknown	Reportedly positive	Positive	Negative	Not tested	Not tested
IV/15	No, deceased	Severe dystonia-parkinsonism and dementia	Early onset (~12 y)	Reportedly positive	Not tested	Not tested	Not tested	Not tested
IV/16	No	No symptoms	N/A	Not performed	Negative	Negative	Not tested	Not tested
V/5	Yes	Psychiatric (depression and delusions; MOCA = 28)	N/A	Negative	Negative	Negative	Not tested	Not tested
V/6	Yes	No symptoms	N/A	Negative	Negative	Negative	Not tested	Not tested

Abbreviations: GP = globus pallidus; MOCA = Montreal Cognitive Assessment; N/A = not applicable; SN = substantia nigra.

Figure 2 Brain MRIs of clinically and radiologically affected family members



Brain MRIs of affected family members are depicted. Every row represents a single patient. (A–D) Patient IV/7. (E–H) Patient III/5. (I–L) Patient III/10. (M–P) Patient IV/11. In the first 2 columns, T2-weighted images of the brain at the level of the substantia nigra and at the level of the basal ganglia are represented. In the second 2 columns, iron-sensitive sequences are represented in the same level. Because MRIs were not performed at the same time point, C, D, G, and H are T2*, whereas K and L are T2-FFE. O and P are derived from susceptibility-weighted imaging sequences. All images show iron accumulation in the substantia nigra and globus pallidus internus. However, in patient III/10 (images I–L), iron accumulation is present in the head of the caudate also, and there is a marked global atrophy. In the index case, a linear hyperintense streaking, indicating internal medullary lamina of the globus pallidus, was also present (arrow in image B).

MLPA detected a *de novo* *PLA2G6* exon duplication. Segregation analysis in 12 family members showed the MPAN variant to be segregating with the disease (figure 1).

Neuropathology

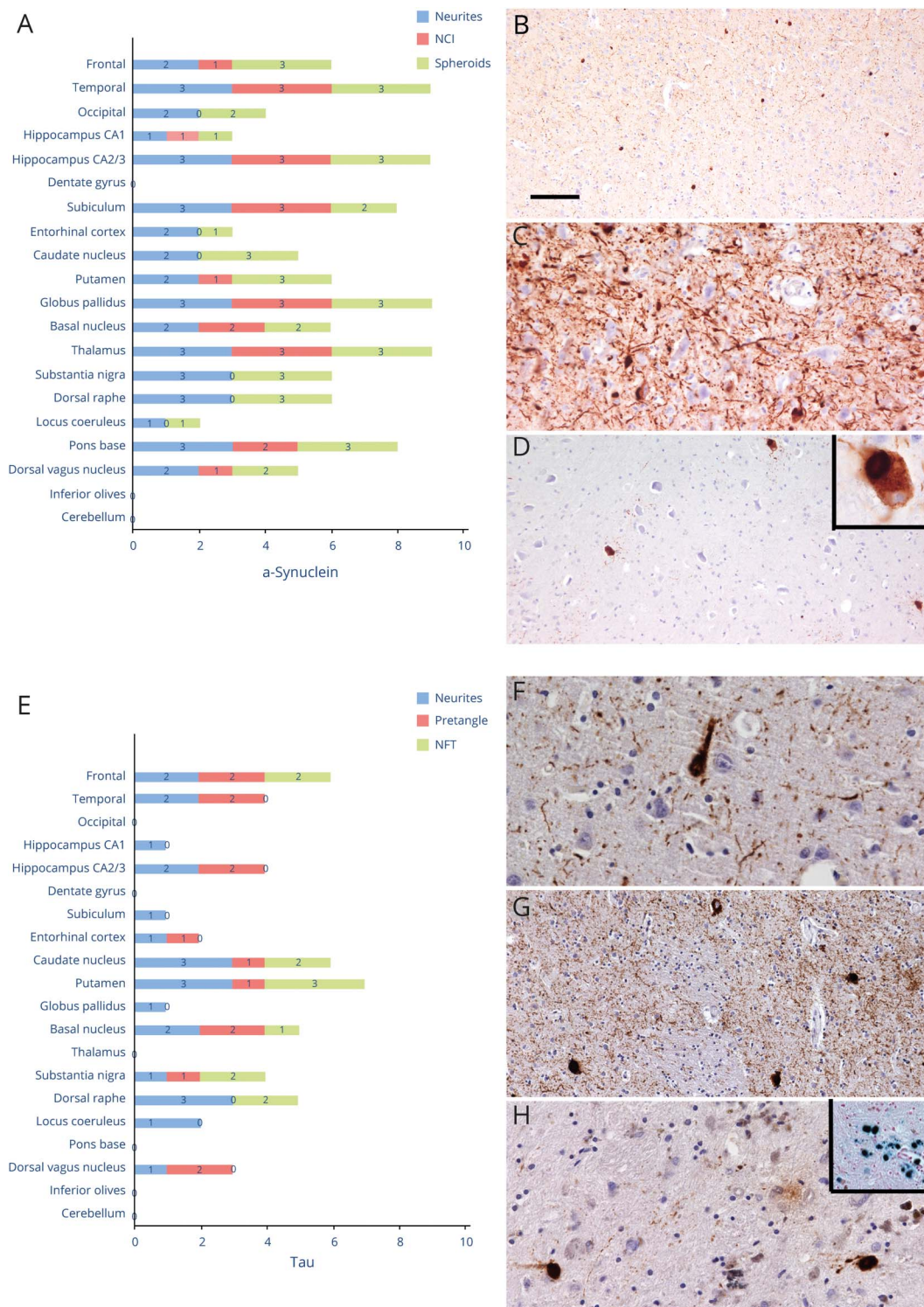
Neuropathologic examination was performed in patient IV/15 (figure 3). Neuronal loss and astrogliosis predominated in the temporal cortex, striatum, globus pallidus, and substantia nigra. Accumulation of Prussian-blue positivity was present in the globus pallidus. APP axonal spheroids predominated in the regions showing prominent neuronal loss, but they were noted in cortical areas as well. TDP-43 and β -amyloid-positive pathologic deposits were absent.

Alpha-synuclein pathology (figure 3, A–D) was characterized by neurites and spherical neuronal cytoplasmic deposits; however, on hematoxylin and eosin staining in the brainstem,

they were not seen as unequivocal Lewy bodies. However, in the cortex, cortical Lewy body–like structures were identified. In all regions, extracellular spherical bodies were also immunostained by alpha-synuclein antibodies. The distribution of alpha-synuclein pathology was also most prominent in the basal ganglia; it was present also in the cortical areas and hippocampus. In the brainstem, neuronal inclusions were observed mostly in the substantia nigra. They were also observed in the dorsal vagus nucleus and as an unusual feature in the inferior olives but not in the locus coeruleus, where only neurites and spheroids were noted. Thus, the distribution of neuronal alpha-synuclein deposition was not exactly compatible with the Braak stages of Lewy pathology.⁶ Glial alpha-synuclein pathology was not present.

Tau pathology (figure 3, E–H) was characterized by neuropil threads, neurites, diffuse neuronal cytoplasmic

Figure 3 Neuropathologic features of an individual from this family (case IV/15)



Anatomic mapping of alpha-synuclein–positive neurites, neuronal cytoplasmic inclusions (NCIs), and spheroids (A). NCIs and neurites in the temporal cortex (B) and the CA2/3 subregion of the hippocampus (C) and NCIs in the inferior olives (D); the upper right inset shows an enlarged neuron. Anatomic mapping of tau-positive neurites, pretangles, and neurofibrillary tangles (NFTs) (E). NFT and neuropil threads/neurites in the frontal cortex (F), putamen (G), and globus pallidus (H); in the globus pallidus iron accumulation as shown in the upper right inset with Prussian-blue staining.

positivity (pretangles), and less neurofibrillary tangles. The distribution of tau pathology did not follow the Braak and Braak stages⁷ and predominated the

basal ganglia, substantia nigra, frontal and temporal cortex, and hippocampus. Glial tau pathology was not observed.

Discussion

Our study serves as additional evidence for dominant inheritance for certain *C19Orf12* variants, possibly through dominant negative effects. The detected *C19Orf12* (heterozygous NM_001031726.3:c.335G>A; p.Trp112Ter) variant causes stop-gain at the same amino acid position as reported by Gregory et al.⁴ in a family with dominant inheritance. The variant detected in our study perfectly segregates with the phenotype in the 12 tested family members. Nonsense-mediated decay is not predicted by the R package “masonmd”⁸; thus, it is very likely that this is the most important pathogenic driver variant in this family. Clinical evidence, which also supports the diagnosis of MPAN, includes psychiatric manifestation in certain family members and the linear streaking⁹ on the MRI in the index patient. However, apparently no family member had axonal neuropathy. Marked intrafamilial phenotypic heterogeneity was detected in this family; that is, certain family members have only mild parkinsonism, whereas others show severe and rapidly deteriorating dystonia-parkinsonism and dementia. Thus, in certain individuals or sporadic cases, heterozygous *C19Orf12* variants may contribute to parkinsonism; however, this observation needs to be proven.

Why marked differences were observed in the expressivity of the disease still remained a question. The frameshift variant detected in the *CP* gene (NM_000096.4:c.313delG; p.Val105PhefsTer5) is missing from the population databases and can be classified as likely pathogenic according to the American College of Medical Genetics and Genomics guideline (evidence: PVS1, PM2). Pathogenic variants in the *CP* genes associate with autosomal recessive cerebellar ataxia and aceruloplasminemia (MIM: 604290).¹⁰ Although aceruloplasminemia is considered an autosomal recessive disease, many reports describe cerebellar ataxia in heterozygous carriers.^{11,12} In these patients, lower serum ceruloplasmin and copper levels are present, and MRI detects cerebellar atrophy. Although the index case had consistently low serum ceruloplasmin (between 0.08 and 0.11 g/L) and copper levels (between 5.8 and 9.0 μmol/L), family members with mild symptoms and without symptoms were also carriers. Therefore, the effect of this variant is ambiguous.

MLPA detected a de novo *PLA2G6* exon 14 duplication in the index case. *PLA2G6* mutations are associated with a diverse clinical spectrum (*PLA2G6*-associated neurodegeneration; MIM: 256600; 610217; 612953). It is difficult to weight the effect of exon 14 duplication in our patient. According to Crompton et al.,¹³ deletion/duplication events may account for up to 12.5% of *PLA2G6* mutations, but whether single heterozygous mutations may lead to any symptoms is controversial. A single case report suggested that heterozygous *PLA2G6* mutation might lead to Parkinson disease 14 (*PARK14*).¹⁴ Of interest, Lewy body pathology is also present in *PLA2G6* associated neurodegeneration (*PLAN*).

The heterozygous *TPPI* variant (NM_000391.4:c.622C>T; p.Arg208Ter) gained our attention because it is a stop-gain

variation and a well-known pathogenic variant (ClinVarID: 2643) in neuronal ceroid lipofuscinosis (*CLN2*; MIM: 204500).¹⁵ It is a variant inherited from the father. *CLN2* is an autosomal recessive disease with severe, progressive neurodegeneration, most commonly starting at age 2–4 years. Clinical symptoms include seizures, loss of speech, impaired psychomotor function, blindness, and premature death. In summary, it is less likely that this variant is directly connected to the phenotype of the described family.

Although the simultaneous presence of rare heterozygous variants on the same disease pathway raises the possibility of oligogenic inheritance in the background of differential expressivity, it is impossible to prove this in a single family. However, such findings are more frequently recognized with the use of next-generation sequencing,¹⁶ so this problem needs to be addressed in the future.

Altogether, there were only 4 autopsy reports from MPAN cases in the literature to date.^{3,4,17} To summarize the findings from these reports, widespread cortical-subcortical alpha-synuclein-positive Lewy pathology was present in both recessive and dominant cases with less pronounced tau pathology, mainly in the hippocampus. Neuropathologic examination of patient IV/15 was partially compatible with these reports; however, we identified some unusual features, most importantly, the pronounced tau pathology was unique in this case. Tau pathology was neuronal and was not compatible with that seen in primary tauopathies or Alzheimer disease.¹⁸ However, it is yet uncertain whether the widespread tau pathology is specific to MPAN. In addition, as an unusual feature, we detected neuronal cytoplasmic alpha-synuclein-positive inclusions in the inferior olives.

In this study, we report one of the largest MPAN families in the literature to date, confirming possible dominant inheritance of this disease. Neuropathologic study of a single family member showed widespread tau pathology beside the characteristic alpha-synucleinopathy. Although oligogenic inheritance was raised as a possibility in the background of differential expressivity, this hypothesis needs to be proven in systematic studies.

Acknowledgment

The authors thank the patients for their participation in this study. Several authors of this publication are members of the European Reference Network for Rare Neurological Diseases: Project ID No. 739510.

Study funding

Supported by the Hungarian Brain Research Program KTIA_NAP_2017-1.2.1-NKP-2017-00002.

Disclosure

The authors report no disclosures. Go to [Neurology.org/NG](https://www.neurology.org/NG) for full disclosures.

Publication history

Received by *Neurology: Genetics* March 30, 2020. Accepted in final form July 27, 2020.

Appendix Authors

Name	Location	Contribution
Peter Balicza, MD, PhD	Institute of Genomic Medicine, Budapest, Hungary	Patient examination, NGS data analysis, and formulation of the manuscript
Renata Bencsik, MSc	Institute of Genomic Medicine, Budapest, Hungary	Performing NGS, Sanger sequencing, and MLPA and review of the manuscript
Andras Lengyel, MD	Motala Hospital, Sweden	Patient examination and formulation of the manuscript
Aniko Gal, PhD	Institute of Genomic Medicine, Budapest, Hungary	Performing Sanger sequencing and MLPA and review of the manuscript
Zoltan Grosz, MD	Institute of Genomic Medicine, Budapest, Hungary	Patient examination and review of the manuscript
Dora Csaban, MSc	Institute of Genomic Medicine, Budapest, Hungary	Performing NGS and Sanger sequencing and review of the manuscript
Gabor Rudas, MD, PhD	Chair of Neuroradiology, Department of Radiology	Evaluating the brain MRIs and review of the manuscript
Krisztina Danics, MD, PhD	Institute of Forensic Medicine, Budapest, Hungary	Brain pathology analyses and review of the manuscript
Gabor Kovacs, MD, PhD, FRCPC	University of Toronto, Canada	Brain pathology analyses and formulation of the manuscript
Maria Judit Molnar, MD, PhD	Institute of Genomic Medicine, Budapest, Hungary	Patient examination, data analysis, and formulation of the manuscript

References

1. Wiethoff S, Houlden H. Neurodegeneration with brain iron accumulation. In: *Handbook of Clinical Neurology*. Amsterdam, the Netherlands: Elsevier B.V.; 2018: 157–166.
2. Gregory A, Hayflick S. Neurodegeneration with brain iron accumulation disorders overview. In: *GeneReviews* [Internet]. Seattle, WA: University of Washington, Seattle; 1993.
3. Hogarth P, Gregory A, Krueger MC, et al. New NBIA subtype: genetic, clinical, pathologic, and radiographic features of MPAN. *Neurology* 2013;80:268–275.
4. Gregory A, Lotia M, Jeong SY, et al. Autosomal dominant mitochondrial membrane protein-associated neurodegeneration (MPAN). *Mol Genet Genomic Med* 2019;7:e00736.
5. Vincze A, Kapás I, Molnar MJ, Kovács GG. Clinicopathological variability in neurodegeneration with brain iron accumulation. *Ideggyogy Sz* 2010;63:129–135.
6. Braak H, Del Tredici K, Rüb U, De Vos RAI, Jansen Steur ENH, Braak E. Staging of brain pathology related to sporadic Parkinson's disease. *Neurobiol Aging* 2003;24: 197–211.
7. Braak H, Braak E. Neuropathological staging of Alzheimer-related changes. *Acta Neuropathol* 1991;82:239–259.
8. Hu Z, Yau C, Ahmed AA. A pan-cancer genome-wide analysis reveals tumour dependencies by induction of nonsense-mediated decay. *Nat Commun* 2017;8: 15943.
9. Skowronska M, Kmiec T, Jurkiewicz E, Malczyk K, Kurkowska-Jastrzębska I, Członkowska A. Evolution and novel radiological changes of neurodegeneration associated with mutations in C19orf12. *Parkinsonism Relat Disord* 2017;39: 71–76.
10. Marchi G, Busti F, Lira Zidanes A, Castagna A, Girelli D. Aceruloplasminemia: a severe neurodegenerative disorder deserving an early diagnosis. *Front Neurosci* 2019; 13:325.
11. McNeill A, Pandolfo M, Kuhn J, Shang H, Miyajima H. The neurological presentation of ceruloplasmin gene mutations. *Eur Neurol* 2008;60:200–205.
12. Borges MD, de Albuquerque DM, Lanaro C, Costa FF, Fertrin KY. Clinical relevance of heterozygosis for aceruloplasminemia. *Am J Med Genet B Neuropsychiatr Genet* 2019;180:266–271.
13. Crompton D, Rehal PK, MacPherson L, et al. Multiplex ligation-dependent probe amplification (MLPA) analysis is an effective tool for the detection of novel intragenic PLA2G6 mutations: implications for molecular diagnosis. *Mol Genet Metab* 2010; 100:207–212.
14. Ferese R, Scala S, Biagioni F, et al. Heterozygous PLA2G6 mutation leads to iron accumulation within basal ganglia and Parkinson's disease. *Front Neurol* 2018;9:536.
15. Nickel M, Simonati A, Jacoby D, et al. Disease characteristics and progression in patients with late-infantile neuronal ceroid lipofuscinosis type 2 (CLN2) disease: an observational cohort study. *Lancet Child Adolesc Health* 2018;2:582–590.
16. Keogh MJ, Wei W, Aryaman J, et al. Oligogenic genetic variation of neurodegenerative disease genes in 980 postmortem human brains. *J Neurol Neurosurg Psychiatry* 2018; 89:813–816.
17. Hartig MB, Iuso A, Haack T, et al. Absence of an orphan mitochondrial protein, c19orf12, causes a distinct clinical subtype of neurodegeneration with brain iron accumulation. *Am J Hum Genet* 2011;89:543–550.
18. Kovacs GG. Invited review: neuropathology of tauopathies: principles and practice. *Neuropathol Appl Neurobiol* 2015;41:3–23.